CYBERNETICS AND PHYSICS, VOL. 1, NO. 4, 2012 , 228–236

STATE ESTIMATION OF NON-AUTONOMOUS LURIE SYSTEMS OVER THE LIMITED-BAND COMMUNICATION CHANNEL WITH TIME DELAY AND UNIFORM QUANTIZATION

Boris Andrievsky[1,2,3] **and Alexey Andrievsky**[1]
[1] Control of Complex Systems Lab., The Institute for Problems of Mechanical Engineering of the RAS,
[2] Mathematics and Mechanics Faculty, Saint Petersburg State University,
[3] Control Systems and Informatics Dept., The National Research University of Information Technologies, Mechanics and Optics, Saint Petersburg, Russia
boris.andrievsky@gmail.com, alexey.andrievsky@gmail.com

Abstract
The paper is devoted to the remote state estimation problem for nonlinear non-autonomous Lurie systems over the limited-band communication channel with time delay. Dependence of the transmission error is studied analytically and evaluated experimentally. It is demonstrated that the upper bound for limit estimation error depends linearly on the transmission error which, in turn, is proportional to the driving signal rate and inversely proportional to the transmission rate. The experimental results obtained for the multipendulum setup confirm the theoretical statements.

Key words
State estimation, communication constraints, delay, mechatronic setup.

1 Introduction

The limitations of estimation and control under constraints imposed by a finite capacity information channel have been investigated in detail in the control theoretic literature, see the surveys [Nair *et al.*, 2007; Andrievsky *et al.*, 2010], the monograph [Matveev and Savkin, 2009] and the references therein. It has been shown that stabilization of linear systems under information constraints is possible if and only if the capacity of the information channel exceeds the entropy production of the system at the equilibrium (*Data Rate Theorem*), [Nair and Evans, 2003; Nair and Evans, 2004; Nair *et al.*, 2004].

Continuous-time nonlinear systems were considered in [Liberzon and Hespanha, 2005; De Persis, 2005; De Persis and Isidori, 2004; De Persis, 2006; Cheng and Savkin, 2007], where several sufficient conditions for different estimation and stabilisation problems were obtained. In [De Persis, 2006], uniformly observable systems were considered and an "embedded-observer" decoder and a controller were designed, which semi-globally stabilizes this class of systems under data-rate constraints.

Problem of stabilizability of nonlinear networked systems for continuous-time plant with a globally Lipschitz nonlinearity is addressed in [Savkin, 2005; Savkin and Cheng, 2007], and a criterion of detectability of a nonlinear system via limited capacity communication channels is also obtained, see [Matveev and Savkin, 2009, Chapter 4.1]. Extensions of these results to the case of nonlinear systems with monotonic nonlinearities are given in [Cheng and Savkin, 2007].

In most of the above mentioned works the coding-decoding procedure is rather complicated: the size of the required memory exceeds or equals to the dimension of the system state space. Such a draw-back was overcome in [Fradkov *et al.*, 2006], where a first order coder scheme was proposed for SISO nonlinear autonomous systems, represented in the Lurie form (linear part plus nonlinearity, depending only on measurable outputs) and the limit possibilities of synchronization and state estimation under information constraints were established. Complexity of the scheme of [Fradkov *et al.*, 2006] does not grow with the dimension of the system state.

The results of [Fradkov *et al.*, 2006] have been further extended in [Fradkov *et al.*, 2006; Fradkov *et al.*, 2008; Fradkov and Andrievsky, 2009; Fradkov *et al.*, 2010*b*; Fradkov and Andrievsky, 2011] to the MIMO case. It is shown that the upper bound of the limit estimation error is proportional to the upper bound of the transmission error and, as a consequence, it is proportional to the maximum rate of the coupling signal and inversely proportional to the information transmis-

sion rate. In [Andrievsky and Fradkov, 2012], this data transmission scheme has been modified for non-autonomous systems. In the above-mentioned works by Fradkov *et al.*, the channel imperfections such as transmission delays, packet losses and dropouts were neglected. In the present paper the results of [Andrievsky and Fradkov, 2012] are extended to the case of time-delays in the communication channel. The transmission error is analytically evaluated and the proposed state estimation procedure is experimentally studied for the real-world system, subjected to measurement errors and data losses.

The paper is organized as follows. The state estimation scheme of [Andrievsky and Fradkov, 2012] is recalled in Section 2. Coding procedure is presented in Section 2.1. Main theoretical result of the paper is given in Section 2.2, where the transmission error for the case of a channel with the time- delay is analytically evaluated. The experimental multipendulum setup is briefly presented in Section 3. Results of the experiments are described in Section 4. Concluding remarks are given in Section 5.

2 State Estimation Scheme

Consider a system model in the Lurie form. In addition to [Fradkov *et al.*, 2006; Fradkov *et al.*, 2008; Fradkov and Andrievsky, 2009; Fradkov *et al.*, 2010*b*; Fradkov and Andrievsky, 2011], let us assume presence of an exogenous input signal and consider the following non-autonomous system:

$$\dot{x}(t)=Ax(t)+\varphi\big(y(t)\big)+Bu(t),\ y(t)=Cx(t), \quad (1)$$

where $x(t)\in\mathbb{R}^n$ is the state variables vector; $y(t)\in\mathbb{R}^l$ is the system output; $u(t)\in\mathbb{R}^m$ denotes an exogenous input; A is $(n\times n)$-matrix; B is $(n\times m)$-matrix; C is $(l\times n)$-matrix; $\varphi(y)$ is a continuous nonlinear vector-function, $\varphi:\mathbb{R}^l\to\mathbb{R}^n$. We assume that the system is dissipative: all the trajectories of the system (1) belong to a bounded set Ω (e.g. attractor of a chaotic system). Such an assumption is typical for oscillatory and chaotic systems. Let signals $u(t)$, $y(t)$ be measured at the side of the source system (1) and be transmitted to the remote observer over the digital communication channel.

The observer has the following form:

$$\dot{\hat{x}}(t)=A\hat{x}(t)+\varphi\big(\bar{y}(t)\big) + L\big(\bar{y}(t)-\hat{y}(t)\big)+B\bar{u}(t),\ \hat{y}=C\hat{x}, \quad (2)$$

where $\hat{x}(t)\in\mathbb{R}^n$ is the vector of the state estimates, produced by the observer; $\bar{u}(t)$, $\bar{y}(t)$ are, respectively, plant (1) input and output signals, transmitted over the channel and restored by the decoder; L is the vector of the observer parameters (gain). Apparently, in absence of transmission errors (i.e. if $\bar{u}(t)\equiv u(t)$, $\bar{y}(t)\equiv y(t)$), the dynamics of the state error vector $e(t)=x(t)-\hat{x}(t)$ are described by a linear equation

$$\dot{e}=A_Le,\ y=Cx, \quad (3)$$

where $A_L=A-LC$.

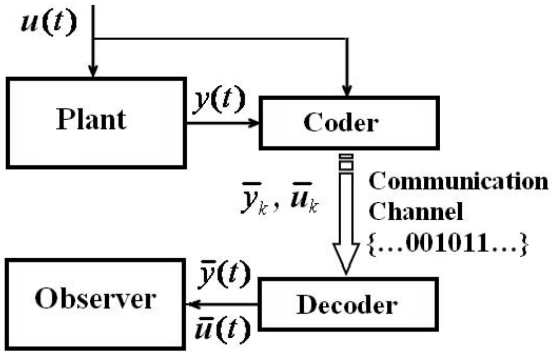

Figure 1. Block-diagram of state estimation over a discrete communication channel.

In the case if the pair (A,C) is observable, there exists L providing the matrix A_L with any given eigenvalues. In particular all eigenvalues of A_L can have negative real parts, i.e. the system (3) can be made asymptotically stable and $e(t)\to 0$ as $t\to\infty$. Therefore, in the absence of measurement and transmission errors the estimation error decays to zero.

Now let us take into account transmission errors. Let observed signals $u_i(t)\in\mathbb{R}^l$, $y_j(t)\in\mathbb{R}^l$ $(i=1,\ldots,m,$ $j=1,\ldots,m)$ be coded with symbols from a finite alphabet at discrete sampling time instants $t_{k,i}=k_iT_{s,i}$, $t_{k,j}=k_jT_{s,j}$ where $T_{s,i}$, $T_{s,j}$ are the sampling periods. Disregarding difference in representation of digital numbers and symbols of the coding alphabet, let us denote the output codewords as $\bar{u}_i[k]=\bar{u}(t_{k,i})$, $\bar{y}_j[k]=\bar{y}(t_{k,j})$ (respectively). The block-diagram, illustating the considered remote estimation scheme is shown in Fig. 1 (cf. [Tatikonda *et al.*, 1998; Tatikonda and Mitter, 2004]).

At the present stage of the study we assume that the observations are not corrupted by the observation noise, and that transmission delay and distortion may be neglected.

Assume that *zero-order extrapolation* is used to convert the digital sequences $\bar{u}_i[k]$, $\bar{y}_j[k]$ $(i=1,\ldots,m,$ $j=1,\ldots,m)$ to the continuous-time input signals $\bar{u}_i(t)$, $\bar{y}_j(t)$ of the observer (2): $\bar{u}_i(t)=\bar{u}_i[k_i]$, $\bar{y}_j(t)=\bar{y}_j[k_j]$ as $k_iT_{s,i}\le t<(k_i+1)T_{s,i}$, $k_jT_{s,j}\le t<(k_i+1)T_{s,j}$. Then the transmission error vectors are as follows:

$$\delta_u(t)=u(t)-\bar{u}(t)\in\mathbb{R}^m,$$
$$\delta_y(t)=y(t)-\bar{y}(t)\in\mathbb{R}^l. \quad (4)$$

In the presence of transmission errors, equation (3) reads as

$$\dot{e} = A_L e + \varphi(y) - \varphi\big(y + \delta_y\big) - B\delta_u - L\delta_y. \quad (5)$$

Let us consider the limitations imposed on the estimation precision by the limitation on the transmission rate. To this end introduce upper bounds on the limit output estimation errors $Q_i = \sup \overline{\lim_{t\to\infty}} \|\varepsilon_i(t)\|$, where $\varepsilon_i(t) = y_i(t) - \hat{y}_i(t)$, $i = 1, \ldots, l$, and the supremum is taken over all admissible transmission errors. In [Fradkov *et al.*, 2006; Fradkov *et al.*, 2008; Andrievsky and Fradkov, 2012] it has been proved analytically and illustrated by numerical examples, that for the considered estimation scheme, applied to an autonomous system, the total estimation error is proportional to the upper bound of the norm of the transmission error and, in turn, is inversely proportional to the transmission rate. It is easy to show that this relationship is also valid for non-autonomous system, if an exogenous signal is transmitted to the observer at the receiver's end by means of the coding-decoding procedure (6), (8), (9). In the next section, the experiments on the mechatronic laboratory setup for evaluation of the estimation error are described. It is shown that the experimental results agree with the general statements of [Fradkov *et al.*, 2006; Fradkov *et al.*, 2008].

2.1 Coding Procedure

Following [Fradkov *et al.*, 2006], for a given real number $\varkappa > 0$ and nonnegative integer $\nu \in \mathbb{Z}$ define a uniform quantizer to be a discretized map $q_{\nu,\varkappa} : \mathbb{R} \to \mathbb{R}$ as follows. Introduce the *range interval* $\mathcal{I} = [-\varkappa, \varkappa]$ of length $2\varkappa$. Let this interval be equally split into 2^ν parts. Define the *discretization interval* of length $\delta = 2^{1-\nu}\varkappa$ and the quantizer $q_{\nu,\varkappa}(z)$ as

$$q_{\nu,\varkappa}(z) = \begin{cases} \delta \cdot \langle \delta^{-1} z \rangle, & \text{if } |z| \le \varkappa, \\ \varkappa \operatorname{sign}(z), & \text{otherwise}, \end{cases} \quad (6)$$

where z denotes the signal to be transmitted over the channel (in our case, $z \in \{u, y\}$), $\langle \cdot \rangle$ denotes round-up to the nearest integer, $\operatorname{sign}(\cdot)$ is the signum function: $\operatorname{sign}(y) = 1$, if $y \ge 0$, $\operatorname{sign}(y) = -1$, if $y < 0$. Therefore, the cardinality of the mapping $q_{\nu,\varkappa}$ image is equal to $2^\nu + 1$, and each codeword symbol contains $\breve{R} = \log_2(2^\nu + 1) = \log_2(2\varkappa/\delta + 1)$ bits. Thus, the discretized output of the considered coder is found as $\bar{z} = q_{\nu,\varkappa}(z)$. We assume that the coder and decoder make decisions based on the same information [Tatikonda *et al.*, 1998; Tatikonda and Mitter, 2004].

In the present paper we use $l + m$ independent coders for components u_i, y_j ($i = 1, \ldots m$, $j = 1, \ldots, l$) of the transmitted vectors $u \in \mathbb{R}^m$, $y \in \mathbb{R}^l$. Each coder number i, j has its particular sampling period $T_{s,i}$, $T_{s,j}$, ranges $\varkappa_i$, $\varkappa_j$ and integers ν_i, ν_j. The corresponding bit-per-second rates R_i, R_j are calculated as $R_i = \breve{R}_i/T_{s,i} = \log_2(2_i^\nu + 1)/T_{s,i}$, $R_j = R_i = \breve{R}_j/T_{s,j} = \log_2(2_j^\nu + 1)/T_{s,j}$. The overall rate R is a sum of the particular ones, $R = \sum_{i=1}^{l} R_i + \sum_{j=1}^{m} R_j$.

The static quantizer (6) is a part of the time-varying coders with memory, see e.g. [Nair and Evans, 2003; Brockett and Liberzon, 2000; Tatikonda and Mitter, 2004; Fradkov *et al.*, 2006]. Two underlying ideas are used for this kind of coder:

- reducing the coder range $\varkappa$ to cover the some area around the predicted value for the $(k+1)$th observation $z[k+1]$, $z[k+1] \in \mathcal{Z}[k+1]$. This means that the quantizer range $\varkappa$ is updated during the time and a time-varying quantizer (with different values of $\varkappa$ for each instant, $\varkappa = \varkappa[k]$) is used. Using such a "zooming" strategy it is possible to increase coder accuracy in the steady-state mode, and, at the same time, to prevent coder saturation at the beginning of the process;
- introducing memory into the coder, which makes it possible to predict the $(k+1)$th observation $z[k+1]$ with some accuracy and, therefore, to transmit over the channel only encrypted innovation signal.

To describe the first-order (one-step memory) coder let us introduce the sequence of central vectors (sequence of "*centroids*") $c[k] \in \mathbb{R}^l$, $k \in \mathbb{Z}$ with initial condition $c[0] = 0$ [Tatikonda and Mitter, 2004]. At step k the coder compares the current measured output $z[k]$ with the number $c[k]$, forming the deviation vector $\partial z[k] = z[k] - c[k]$. Then this vector is discretized with a given $\varkappa = \varkappa[k]$ according to (6). The output signal

$$\bar{\partial} z[k] = q_\varkappa(\partial z[k]) \quad (7)$$

is represented as an $\breve{R}$-bit information symbol from the coding alphabet and transmitted over the communication channel to the decoder. Then the central number $c[k+1]$ and the range parameter $\varkappa[k]$ are renewed based on the available information about the drive system dynamics. Assuming that the transmitted signal $z(t)$ changes at a slow rate, i.e. that $z[k+1] \approx z[k]$. we use the following update algorithms:

$$c[k+1] = c[k] + \bar{\partial} z[k], \quad c[0] = 0, \quad (8)$$

$$\varkappa[k] = (\varkappa_0 - \varkappa_\infty)\rho^k + \varkappa_\infty, \ \ k = 0, 1, \ldots, \quad (9)$$

where $0 < \rho \le 1$ is the decay parameter, $\varkappa_\infty$ stands for the limit value of $\varkappa$. The initial value $\varkappa_0$ should be large enough to capture all the region of possible initial values of z_0.

Equations (6), (7), (9) describe the coder algorithm. A similar algorithm is used by the decoder. Namely: the sequence of $\varkappa[k]$ is reproduced at the receiver node

utilizing (9); the values of $\bar{\partial}z[k]$ are restored with given $\varkappa[k]$ from the received codeword; the central numbers $c[k]$ are found in the decoder in accordance with (8). Then $\bar{z}[k]$ is found as a sum $c[k]+\bar{\partial}z[k]$.

2.2 Main Theoretical Result. Evaluation of the Estimation Error

Denoting in the right hand of (5) the sum $\varphi(y)-\varphi\big(y+\delta_y\big)-B\delta_u-L\delta_y$ as $\xi(t)\in\mathbb{R}^n$, one obtains the followng observer error equation:

$$\dot{e}(t)=A_Le(t)+\xi(t), \tag{10}$$

where $\xi(t)$ is l_2-norm bounded disturbing vector, $\|\xi(t)\|\le C_\xi$, where $C_\xi\ge 0$ depends on the magnitudes of $\delta_y(t)$, $\delta_u(t)$, on function $\varphi(\cdot)$ and matrices A, B. Namely, assuming that a nonlinearity $\varphi(\cdot)$ is Lipschitz continuous along all the trajectories of the observed system (1), i.e. that there exists a positive real number $L_\varphi>0$ such that $\|\varphi(y)-\varphi\big(y+\delta_y\big)\|\le L_\varphi\|\delta_y\|$, one may majorize C_ξ as $C_\xi\ge(L_\varphi+\|L\|)\|\delta_y\|+\|B\|\cdot\|\delta_u\|$.

Let us evaluate the magnitudes $\|\delta_u\|$, $\|\delta_y\|$ of the *transmission errors* $\delta_u(t)$, $\delta_y(t)$. Since all the components $u_i(t)$ $(i=1,\dots,m)$, $y_j(t)$ $(j=1,\dots,l)$ are transmitted over the channel by means of scalar coding–decoding procedures (6)–(9), let us denote the scalar signal to be transmitted as $z(t)$ and evaluate the upper bound $\Delta_z=\sup\overline{\lim_{t\to\infty}}|\delta_z(t)|$ of the data transmission error $\delta_z(t)=z(t)-\bar{z}(t)$. To this end let us follow the lines of [Fradkov *et al.*, 2006; Andrievsky and Fradkov, 2012], additionally taking into account transmission delay τ. In the present study it is assumed that τ is a given nonnegative constant and, for the sake of conciseness, that the time delay is uniform for all channels.

Let the growth rate of $z(t)$ be uniformly bounded, i.e. there exists a positive real number L_z such as $\sup\limits_t|\dot{z}(t)|\le L_z$. Let bit-per-second rate R, parameter $\nu\in\mathbb{Z}$, and range parameter κ of quantizer (6) be given parameters (chosen by the designer). The aim is to find an upper bound of the transmission error Δ_z as a function of R, κ and L_z. Note that quantizer range κ can not be arbitrarily chosen, cf. (20).

The *quantization interval* δ of quantizer (6) is defined as

$$\delta=2^{1-\nu}\kappa. \tag{11}$$

As follows from (6), the magnitude of the quanization error $\delta_{\partial z}=\partial z-\bar{\partial z}$ (where $\partial z[k]=z[k]-c[k]$, $\bar{\partial z}=q_{\nu,\kappa}(\partial z)$) for given ∂z does not exceed $\delta/2=2^{-\nu}\kappa$, if

$$|\partial z|\le\kappa+\delta/2=(1+2^{-\nu})\kappa. \tag{12}$$

Inequality (12) corresponds to the nonsaturated quantization, e.g. to the "*nominal case*". If (12) is violated, then the error grows linearly on ∂z. Therefore the magnitude of the quantization error $\delta_{\partial z}$ satisfies the inequality

$$|\delta_{\partial z}|\le\begin{cases}2^{-\nu}\kappa, & \text{if } |\partial z|\le(1+2^{-\nu})\kappa,\\ |\partial z-\kappa| & \text{otherwise.}\end{cases} \tag{13}$$

The bit-per-step rate $\breve{R}$ for quantizer (6) is given by the following expression:

$$\breve{R}=\log_2(2^\nu+1). \tag{14}$$

Since the bit-per-second rate R may be found as $R=\breve{R}/T_s$, where T_s denotes the sampling period, it is valid the following expression for T_s in the terms of the other coder parameters (see Fig. 2):

$$T_s=\log_2(2^\nu+1)R^{-1}. \tag{15}$$

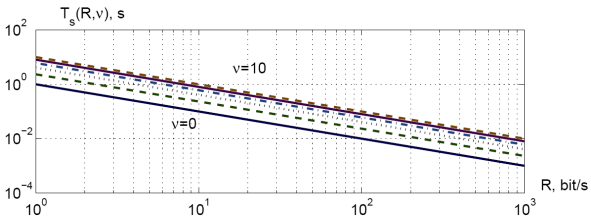

Figure 2. Sampling time T_s versus coder parameter ν and bit-per-second rate R. Solid lines: $\nu=0$, $\nu=8$; dashed lines: $\nu=2$, $\nu=10$; dotted line: $\nu=4$, dash-dot line: $\nu=6$.

Now let us turn to procedure (8) of updating the central number. Firstly, assume, that at k-th step the measured value $z[k]=z(t_k)$, $t_k=kT_s$, belongs to the interval $[-\kappa-\delta/2,\kappa+\delta/2]$ around the central number $c[k]$:

$$|z[k]-c[k]|\le\kappa+2^{-1}\delta. \tag{16}$$

This means fulfillment of inequality (12). Therefore in this case the quantization error $\delta_{\partial z}$ does not exceed $2^{-\nu}\kappa$. According to update algorithm (8), the next value of the central number is found as

$$c[k+1]=c[k]+\bar{\partial}z[k]. \tag{17}$$

Apparently, $c[k+1]$ represents $z[k]$ with a maximal error $2^{-\nu}\kappa$, i.e. $|c[k+1]-z[k]|\le 2^{-\nu}\kappa$. To ensure the nonsaturated mode of the coder, inequality (16) should

be valid at the next step $k := k + 1$. This may be guaranteed if the quantizer range κ is sufficiently large for given $L_z \geq \sup_t |\dot{z}|$. Since $|z(t_{k+1}) - z(t_k)| \leq L_z(T_s+\tau)$, then κ should satisfy the following inequality:

$$\kappa \geq L_z(T_s + \tau). \tag{18}$$

Consider now the case when (16) is violated for some $k = k_0$. In this case the quantization error may be large depending on $c[k_0]$, see (13). However, it may be easily shown that if the quantizer range κ satisfies inequality (18) with some margin, i.e. if κ is taken as

$$\kappa \geq (1 + \theta)(T_s + \tau)L_z, \tag{19}$$

where $\theta > 0$ is an arbitrary small real number, then there exists an integer $k_0 < k^* < \infty$ such that (16) is fulfilled for all k, starting from $k = k^*$. If $\theta = 0$ is taken in (19), then only asymptotic convergence may be ensured. In what follows, we assume that validity of (17) is assured by means of an appropriate choise of $\kappa[0]$ in zooming procedure (9).

It follows from (15), (18) that κ should satisfy the relation:

$$\kappa \geq L_z\big(\log_2(2^\nu + 1)R^{-1} + \tau\big). \tag{20}$$

To analyze the coder-decoder accuracy let us evaluate the upper bound $\Delta_z = \sup_t \|\delta_z(t)|$ of the transmission error $\delta_z(t) = z(t) - \bar{z}(t)$. Consider the sampling interval $[t_k, t_{k+1}]$, $t_k = kT_s$. It is shown above that $|\delta_z(t_k)|$ does not exceed $\delta/2 = 2^{-\nu}\kappa$. Additionally, the error may increase from t_k to t_{k+1} due to a change of $z(t)$ by a value not exceeding $L_z(T_s + \tau)$ [Fradkov *et al.*, 2006]. Therefore the total transmission error for each interval $[t_k, t_{k+1}]$ meets the inequality $|\delta_z(t_k)| \leq 2^{-\nu}\kappa + L_z(T_s + \tau)$ and Δ_z may be found as

$$\Delta_z = 2^{-\nu}\kappa + L_z(T_s + \tau). \tag{21}$$

Taking into account expression (15) for the sampling period T_s, we obtain the following relation between the transmission error and other parameters:

$$\Delta_z = 2^{-\nu}\kappa + L_z\big(\log_2(2^\nu + 1)R^{-1} + \tau\big), \tag{22}$$

where κ should satisfy (20). To minimize the transmission error for a given rate, a minimal admissible value for κ should be picked up. This implies the following expressions for κ and Δ_z:

$$\kappa = L_z\big(\log_2(2^\nu + 1)R^{-1} + \tau\big), \tag{23}$$

$$\Delta_z = L_z\big(1 + 2^{-\nu}\big)\big(\log_2(2^\nu + 1)R^{-1} + \tau\big). \tag{24}$$

Expressions (23), (24) lead to the following relation between Δ_z and κ:

$$\Delta_z = \big(1 + 2^{-\nu}\big)\kappa, \quad \kappa = \frac{2^\nu}{1 + 2^\nu}\Delta_z. \tag{25}$$

Defining a multiplier $\lambda(\nu)$ as $\lambda(\nu) = \big(1 + 2^{-\nu}\big)\log_2(2^\nu + 1)$ let us rewrite (22) in the following form

$$\Delta_z = L_z\left(\frac{\lambda(\nu)}{R} + \tau\right). \tag{26}$$

Let us find ν minimizing Δ_z for given L_z, R, τ. The derivative of $\lambda(\nu)$ on ν

$$\frac{d\,\lambda}{d\,\nu} = \frac{2^\nu - \ln(2^\nu + 1)}{2^\nu}\ln(2) \tag{27}$$

is strictly positive. Therefore, $\lambda(\nu)$ strictly grows on ν, and Δ_z is minimized at $\nu = 0$. This means optimality of the *binary* quantizer $q_{\nu,\varkappa}(z) = \nu\,\mathrm{sign}(z)$ in the sence of the transmission error for given rate R (cf. [Li and Baillieu, 2004; Fradkov *et al.*, 2006]).

Dependence of the relative error $\Delta_z L_z^{-1} = \lambda(\nu)R^{-1}$ on transmission rate R for $\nu = 0, 2, \ldots, 10$ and $\tau = 0$ is depicted in Fig. 3. The corresponding plot for $\tau = 0.2$ s is shown in Fig. 4. As follows from (24), the relative transmission error linearly grows on transmission delay τ, as demonstrated in Fig. 5, where the mesh-plots of $\Delta_z L_z^{-1}$ versus rate R and time delay τ for $\nu = 2$ and $\nu = 10$ are depicted.

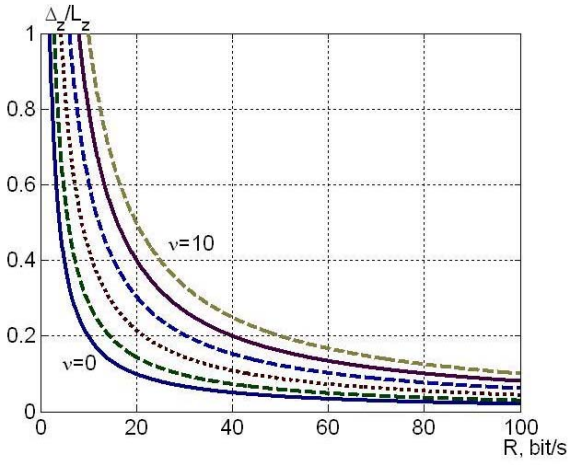

Figure 3. Relative transmission error $\Delta_z L_z^{-1}$ vs rate R. Solid lines: $\nu = 0, \nu = 8$; dashed lines: $\nu = 2, \nu = 10$; dotted line: $\nu = 4$, dash-dot line: $\nu = 6$; $\tau = 0$ s.

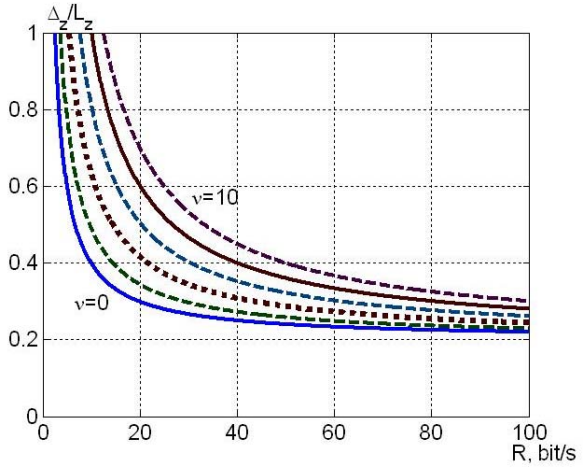

Figure 4. Relative transmission error $\Delta_z L_z^{-1}$ vs rate R. Solid lines: $\nu = 0, \nu = 8$; dashed lines: $\nu = 2, \nu = 10$; dotted line: $\nu = 4$, dash-dot line: $\nu = 6$; $\tau = 0.2$ s.

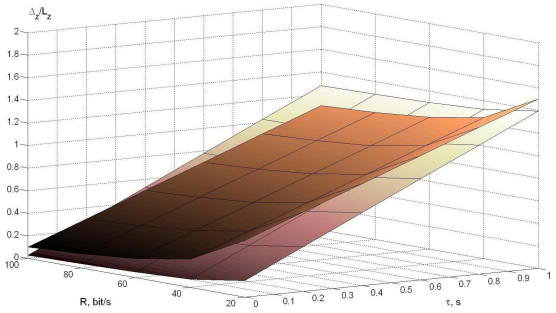

Figure 5. (Color online). Dependence of relative transmission error $\Delta_z L_z^{-1}$ on rate R and time delay τ for $\nu = 2$ (pink) and $\nu = 10$ (copper).

It should be mentioned that, as follows from (26), the total transmission error less than $L_z\tau$ can not be assured.

An experimental evaluation of the accuracy for the described state estimation scheme is presented in the next section.

3 Experimental Setup

The Multipendulum Mechatronic Setup of the IPME RAS (MMS IPME) [Fradkov *et al.*, 2010*a*; Fradkov *et al.*, 2012] consists of the set of interconnected pendulum sections, electrical equipment (with the computer interface facilities), the electric computer-controlled motor, the personal computer for data processing and real-time representation of the results. The mechanical part of the setup consists of a number of identical sections with pendulums, diffusively connected by torsion springs. The computer-controlled electric motor is connected with the first pendulum of the chain via the spring, applying the torque to the "left" end of the chain. The "right" end of the chain is unconnected. Axes of the neighboring sections are connected by torsion springs, arranging force interaction between pendulums. In principle, any number of sections can be connected. At the moment mechanical parts of 50 sections are manufactured. The photo of chain of pendulums and the electric motor is given in Fig. 6.

The pendulum sections and the electric motor are equipped with the electronic modules, providing data exchange with the central computer over the data bus, generation of control signal for the electric motor and data processing of the measured signals. The electronic modules have following functions: data exchange with the data bus, generation of control signals for the electric motor, processing the sensor signals.

On the rotation axis of each pendulum the optical encoder disk for measuring the angle of the pendulum rotation is mounted. The disk has 90 slits. The peripheral part of the disk is posed into the slit of the sensor support. The sensor consists of a radiator (emitting diode) and a receiver (photodiode). The obtained sequences of signals allow to measure angle and the sign of the pendulum angular, and to evaluate amplitude and crossing times and other variables related to the pendulum dynamics. The *angular displacement* and the *driving direction* of the bob are measured by means of the angular encoder, mounted in alignment with the pendulum axis. Pulse patterns from the output of the encoder are transformed by the logical units of the electronic modules into binary codes, which may be read out under data bus requests.

The setup is described in more details in [Fradkov *et al.*, 2010*a*; Fradkov *et al.*, 2012].

Figure 6. Photo of the chain pendulums and the motor.

4 Experiments on State Estimation over the Communication Channel

4.1 Modeling the Chain of Pendulums

Following [Andrievsky and Fradkov, 2009], the *rotation angle* of the drive shaft, connected with the first pendulum of the chain, is considered as the system input. The last (Nth) pendulum in the chain is mechanically connected only with the previous one, no boundary conditions for Nth pendulum are specified. This

leads to the following model of the chain dynamics:

$$\begin{cases} \ddot{\varphi}_1+\rho\dot{\varphi}_1+\Omega^2\sin\varphi_1-k(\varphi_2-2\varphi_1)=ku(t), \\ \dots \\ \ddot{\varphi}_i+\rho\dot{\varphi}_i+\Omega^2\sin\varphi_i-k(\varphi_{i+1}-2\varphi_i+\varphi_{i-1})=0 \\ \qquad (i=2,3,\dots,N-1), \\ \dots \\ \ddot{\varphi}_N+\rho\dot{\varphi}_N+\Omega^2\sin\varphi_N-k(\varphi_N-\varphi_{N-1})=0, \end{cases} \tag{28}$$

where $\varphi_i=\varphi_i(t)$ ($i=1,\,2,\,\dots,N$) are the pendulum deflection angles; $u=u(t)$ is the controlling action (the rotation angle of the drive shaft). The values ρ, ω_0, k are the system parameters: ρ is the viscous friction parameter; Ω is the natural frequency of small oscillations of the isolated pendulum; k is the coupling strength parameter, which depends on the stiffness of the connecting spring. The model (28) parameters have been preliminary estimated based on the mass-geometry properties of the mechanical system, and then were specified by means of the trial-and-error procedure, applied to the experimental data sets. The following parameter estimates were finally obtained: $\Omega = 5.5\ \text{s}^{-1}$, $\rho = 0.95\ \text{s}^{-1}$, $k = 5.8\ \text{s}^{-2}$.

4.2 Data Transmission and State Estimation Algorithms for Multi-pendulum Set-up

In our experiments, the chain of four pendulum sections and the motor, attached via the spring to pendulum #1 were used. The outside left rotary angle (the angle of the drive shaft) may be reffered to as *exogenous* action, applied to the plant (the chain of the pendulums), it was coded by means of the first-orded coder (6), (9), (8), where $z\equiv\varphi_m$ is taken. The model (28) is used for designing the remote state estimator (2), (6), (9), (8) for the pendulum angles $\varphi_i(t)$. Namely, in (6), (9), (8) $z=\varphi_i$ for $i=1,\dots,4$ is taken.

For the considered problem, observer (2) has been designed by means of (28) decomposition into four interconnected subsystems of the second order. This led to the following observer equations:

$$\begin{cases} \dot{\hat{\varphi}}_1=\hat{\omega}_1+l_1\bar{\varepsilon}_1, \\ \dot{\hat{\omega}}_1=-\rho\hat{\omega}_1-\Omega^2\sin\bar{\varphi}_1+k(\hat{\varphi}_2-2\hat{\varphi}_1) \\ \qquad +k\bar{\varphi}_m(t)+l_2\bar{\varepsilon}_1, \\ \dot{\hat{\varphi}}_2=\hat{\omega}_2+l_1\bar{\varepsilon}_2, \\ \dot{\hat{\omega}}_2=-\rho\hat{\omega}_2-\Omega^2\sin\bar{\varphi}_2 \\ \qquad +k(\hat{\varphi}_3-2\hat{\varphi}_2+\hat{\varphi}_1)+l_2\bar{\varepsilon}_2, \\ \dot{\hat{\varphi}}_3=\hat{\omega}_3+l_1\bar{\varepsilon}_3, \\ \dot{\hat{\omega}}_3=-\rho\hat{\omega}_3-\Omega^2\sin\bar{\varphi}_3 \\ \qquad +k(\hat{\varphi}_4-2\hat{\varphi}_3+\hat{\varphi}_2)+l_2\bar{\varepsilon}_3, \\ \dot{\hat{\varphi}}_4=\hat{\omega}_4+l_1\bar{\varepsilon}_4, \\ \dot{\hat{\omega}}_4=-\rho\hat{\omega}_4-\Omega^2\sin\bar{\varphi}_4 \\ \qquad +k(\hat{\varphi}_3-\hat{\varphi}_4)+l_2\bar{\varepsilon}_2, \end{cases} \tag{29}$$

where $\hat{\varphi}_i$, $\hat{\omega}_i$ ($i=1,\dots,4$) stand for the estimates of the rotation angle and the angular velocity of the i-th pendulum (respectively), $\bar{\varepsilon}_i=\bar{\varphi}_i-\hat{\varphi}_i$ are the observer output errors; l_1, l_2 are the oserver gains. To find them, an isolated linear subsystem with the matrices $A_1=\begin{bmatrix}0 & 1\\ -2k & -\rho\end{bmatrix}$, $C_1=[1,0]$ was considered. The gains l_1, l_2 have been found ensuring the prescribed eigenvalues $s_{1,2}=-14\pm 14i$ (where i is an imaginary unit) of the matrix A_1-LC_1, $L=[l_1,l_2]^{\text{T}}$. This gives the following values of the observer gains l_1, l_2: $l_1=27.3$, $l_2=362$. It may be easily verified that for the chosen parameters, the spectrum of the matrix A_L in (5) is as follows: $\{-14.14\pm 13.75i, -14.14\pm 13.93i, -14.14\pm 14.45i, -14.14\pm 14.21i\}$, which leads to exponential stability of observer (2).

4.3 Experimental Results

In course of the experiments, the harmonic waveform voltages have been applied to the motor. The rotary angles of the drive shaft and the pendulums were measured with the sampling rate of 100 Hz and 2^o precision by means of the optical sensors. Then the measured signals have been processed by the above coding algorithms for transferring over the channel. During the experiments, the sampling times for the drive motor T_m and the pendulum angles $T_{\varphi,i}$ and the quantizer (6) parameters ν_i were taken equal: $T_m=T_{\varphi,1}=\dots=T_{\varphi,4}$, $\nu_m=\nu_1=\dots=\nu_4$, varying from one data processing run to another.

Each experiment lasted in $t_{\text{fin}}=100$ s. The relative output estimation errors $Q_i(R,\nu)$ ($i=1,\dots,4$) have been calculated as

$$Q_i(R,\nu)=\frac{\max\limits_{t\in[t_{beg},t_{fin}]}|y_i(t)-\hat{y}_i(t)|}{\max\limits_{t\in[t_{beg},t_{fin}]}|y_i(t)|},$$

where $t_{\text{beg}}=10$ s is taken to eliminate influence of transients on the accuracy indeces $Q_i(R,\nu)$.

Experimental results are depicted in Figs. 7–11. The time histories of the rotation angle of the first pendulum $\varphi_{1,\text{exp}}(t)$, obtained by the experiment, and its estimate $\hat{\varphi}_1(t)$, produced by observer (29) at the decoder's side, are plotted in Figs. 7, 8 for $\nu=0$ (binary coder) and for $\nu=2$. Corresponding estimates $\hat{\dot{\varphi}}_1$ of the angular velocity $\dot{\varphi}_1$ are shown in Figs. 9, 10. It should be noticed, that the the angular velocities are not measured by sensors and are subjected to estimation.

The generalized accuracy indeces are plotted in Figs. 11, 12, where dependence of limit output estimation error for the first pendulum Q_1 on the overall transmission rate R_Σ and parameter ν is reflected. It is worth mentioning that the "exact" values of $\varphi_m(t)$, $\varphi_i(t)$ are not known due to the measuring errors in the optical sensors, effecting on experimental evaluation of the data transmission accuracy. Namely, the overall error can not be less than the optical sensor error. It is

seen from the plots that dependence of the estimation error, obtained by the experiments, are close to the biased inversely proportional function on the transmission rate. One also may notice that small values of ν are preferrable from the viewpoint of the transmission rate for a given accuracy, cf. [Li and Baillieu, 2004; Fradkov *et al.*, 2006].

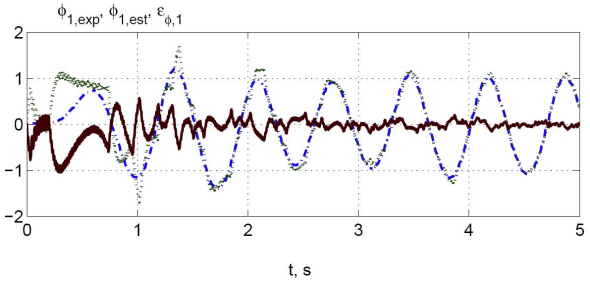

Figure 7. Time histories of $\varphi_{1,\text{exp}}(t)$,$\hat{\varphi}_1(t)$ and output estimation error $\varepsilon_1(t)$. Binary coder. $R_\Sigma = 1.3$ Kbit/s.

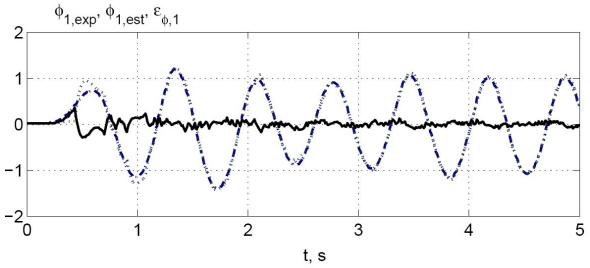

Figure 8. Time histories of $\varphi_{1,\text{exp}}(t)$,$\hat{\varphi}_1(t)$ and output estimation error $\varepsilon_1(t)$. $\nu = 2$. $R_\Sigma = 3.0$ Kbit/s.

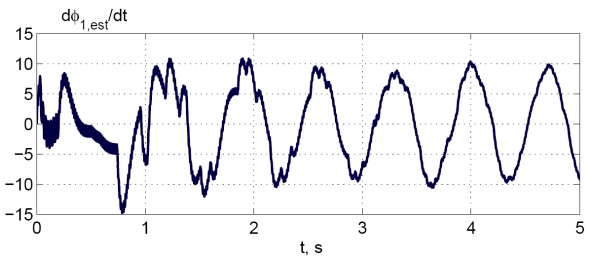

Figure 9. Time history of the angular velocity estimate $\hat{\dot{\varphi}}_1(t)$. Binary coder. $R_\Sigma = 1.3$ Kbit/s.

5 Conclusions

Dependence of the error of state estimation for nonlinear Lurie systems over a limited-band communication channel with delay is analytically studied. It is demonstrated that upper bound for limit estimation error depend linearly on the transmission error which, in turn, is proportional to the driving signal rate and inversely proportional to the transmission rate. The experimental results for remote state estimation of non-autonomous oscillating system (the multipendulum setup) are presented, confirming the theoretical statements.

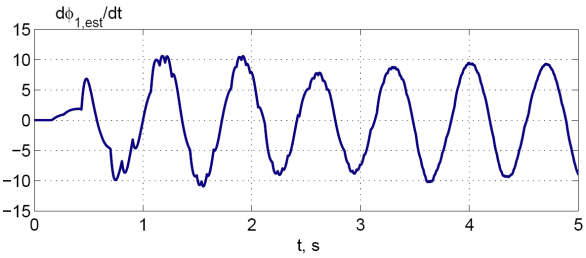

Figure 10. Time history of the angular velocity estimate $\hat{\dot{\varphi}}_1(t)$. $\nu = 2$. $R_\Sigma = 3.0$ Kbit/s.

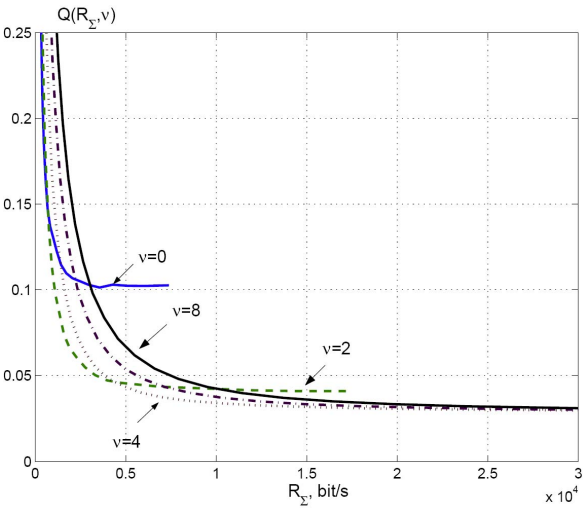

Figure 11. Q_1 vs R for different ν. Solid line: $\nu = 0.8$, dashed line: $\nu = 2$, dotted line: $\nu = 4$, dash-dot line: $\nu = 6$.

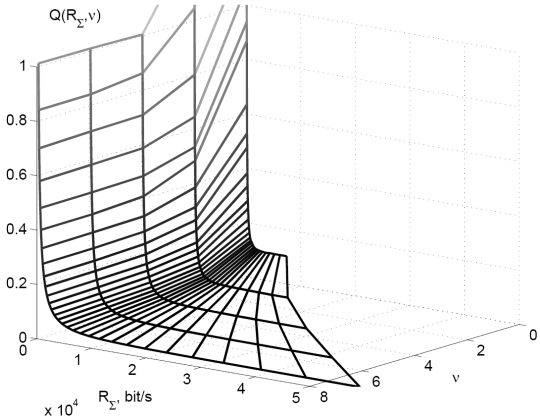

Figure 12. Meshplot of Q_1 vs R, ν.

Acknowlegements

The work was partially supported by the Russian Foundation for Basic Research (project No 11-08-01218, 12-08-01183) and by the Russian Federal Program “Cadres” (agreements 8846,8855).

References

Andrievsky, B., and Fradkov, A.L. (2009) Behavior analysis of harmonically forced chain of pendulums. In: *IEEE International Conference on Control Applications (CCA ’09)*. Saint Petersburg, Russia, pp. 1563–1567.

Andrievsky, B., and Fradkov, A.L. (2012) State estimation of complex oscillatory system with uniform quantization under data rate constraints. In: *Proc. 2012 IEEE Int. Conf. Control Applications (CCA)*, Dubrovnik, Croatia, pp. 865–870.

Andrievsky, B.R., Matveev, A.S., and Fradkov A.L. (2010) Control and estimation under information constraints: Toward a unified theory of control, computation and communications. *Autom. Remote Control* **71**(4), pp. 572–633.

Brockett, R. W., and Liberzon, D. (2000) Quantized feedback stabilization of linear systems. *IEEE Trans. Automat. Contr.* **45**(7), pp. 1279–1289.

Cheng, T.M., and Savkin, A.V. (2007) Output feedback stabilisation of nonlinear networked control systems with non-decreasing nonlinearities: A matrix inequalities approach. *Int. J. Robust Nonlinear Control* **17**, pp. 387–404.

De Persis, C. (2005) n-Bit stabilization of n-dimensional nonlinear systems in feedforward form. *IEEE Trans. Automat. Contr.* **50**(3), pp. 299–311.

De Persis, C. (2006) On stabilization of nonlinear systems under data rate constraints using output measurements. *Int. J. Robust Nonlinear Control* **16**, pp. 315–332.

De Persis, C., and Isidori A. (2004) Stabilizability by state feedback implies stabilizability by encoded state feedback. *Systems & Control Letters* **53**, pp. 249–258.

Fradkov, A.L., and Andrievsky B. (2009) State estimation of passifiable Lurie systems via limited-capacity communication channel. In: *35th Annual Conference of the IEEE Industrial Electronics Society, IECON 2009*. Porto, Portugal, pp. 3039–3044.

Fradkov, A. L., Andrievskiy, B., Boykov, K.B., and Lavrov B.P. (2010*a*) Multipendulum mechatronic setup for studying control and synchronization. In: *Dynamics and control of hybrid mechanical systems. World Scientific Series on Nonlinear Science, Series B – Vol. 14* (G. Leonov, H. Nijmeijer, A. Pogromsky and A. Fradkov, Eds.), pp. 211–222. World Scientific. Singapore.

Fradkov, A. L., Andrievsky, B., and Evans R.J. (2006) Chaotic observer-based synchronization under information constraints. *Physical Review E* **73**, pp. 066209.

Fradkov, A.L., Andrievsky, B., and Evans, R.J. (2008) Hybrid quantised observer for multi-input-multi-output nonlinear systems. In: *Proc. 17th IEEE Int. Conf. Control Applications (CCA 2008)*. San Antonio, Texas, USA, pp. 1195–1200.

Fradkov, A.L., and Andrievsky, B. (2011) Passification based synchronization of nonlinear systems under communication constraints. In: *Prepr. 18th IFAC World Congress*. IFAC. Milano, Italy, pp. 6562–6566.

Fradkov, A.L., Andrievskiy, B., Boykov, K.B., and Lavrov, B.P. (2010*b*) Multipendulum mechatronic setup for studying control and synchronization. In: *Dynamics and control of hybrid mechanical systems, Series on Nonlinear Science, Series B, Vol. 14*, pp. 211–222. World Scientific. Singapore.

Fradkov, A.L., Andrievsky, B., and Boykov, K.B. (2012) Multipendulum mechatronic setup: Design and experiments. *Mechatronics* **22**(1), pp. 76 – 82.

Li, K., and Baillieu, J. (2004) Robust quantization for digital finite communication bandwidth (DFCB) control. *IEEE Trans. Automat. Contr.* **49**(9), pp. 1573–1584.

Liberzon, D., and Hespanha, J.P. (2005) Stabilization of nonlinear systems with limited information feedback. *IEEE Trans. Automat. Contr.* **50**(6), pp. 910–915.

Matveev, A.S., and Savkin, A.V. (2009) *Estimation and Control over Communication Networks*. Birkhäuser. Boston.

Nair, G.N., and Evans, R.J. (2003) Exponential stabilisability of finite-dimensional linear systems with limited data rates. *Automatica* **39**, pp. 585–593.

Nair, G.N., and Evans, R.J. (2004) Stabilizability of stochastic linear systems with finite feedback data rates. *SIAM J. Control Optim* **43**(2), pp. 413–436.

Nair, G. N., Fagnani, F., Zampieri, S., and Evans, R.J. (2007) Feedback control under data rate constraints: an overview. *Proc. IEEE* **95**(1), pp. 108–137.

Nair, G.N., Evans, R.J., Mareels, I.M.Y., and Moran, W. (2004) Topological feedback entropy and nonlinear stabilization. *IEEE Trans. Automat. Contr.* **49**(9), pp. 1585–1597.

Savkin, A.V. (2005) Detectability and output feedback stabilizability of nonlinear networked control systems. In: *Proc. 44th IEEE Conference on Decision and Control*. IEEE. Sevilla, Spain, pp. 8174–8178.

Savkin, A.V., and Cheng, T.M. (2007) Detectability and output feedback stabilizability of nonlinear networked control systems. *IEEE Trans. Automat. Contr.* **52**(4), pp. 730–735.

Tatikonda, S., Sahai, A., and Mitter, S. (1998) Control of LQG systems under communication constraints. In: *Proc. 37th IEEE Conference on Decision and Control*. Vol. WP04. IEEE. Tampa, Florida USA, pp. 1165–1170.

Tatikonda, S., and Mitter, S. (2004) Control under communication constraints. *IEEE Trans. Automat. Contr.* **49**(7), pp. 1056–1068.